Acoustic emissions and electric signal recordings, when cement mortar beams are subjected to three-point bending under various loading protocols

A. Kyriazopoulos
Laboratory of Electronic Devices and Materials, Technological Educational Institute of Athens, 12210, Athens, Greece.
akyriazo@teiath.gr

ABSTRACT. Two experimental techniques are used study the response of cement mortar beams subjected to three-point bending under various loading protocols. The techniques used are the detection of weak electric current emissions known as Pressure Stimulated Currents and the Acoustic Emissions (in particular, the cumulative AE energy and the b-value analysis). Patterns are detected that can be used to predict upcoming fracture, regardless of the adopted loading protocol in each experiment. The experimental results of the AE and PSC techniques lead to the conclusion that when the calculated I_b values decrease, the PSC starts increasing strongly.

KEYWORDS. Pressure Stimulated Currents; Acoustic Emissions; Cement mortar; Three point bending; b-value.

Citation: Kyriazopoulos, A., Acoustic emissions and electric signal recordings, when cement mortar beams are subjected to three point bending under various loading protocols, Frattura ed Integrità Strutturale, 40 (2017) 52-60.
Received: 05.01.2017
Accepted: 26.02.2017
Published: 01.04.2017

INTRODUCTION

The mechanical behavior and the evolution of damage in heterogeneous materials under compressive loading are of great interest in a wide range of application fields. Particularly, the Service Life of cement-based structures deteriorates due to heavy loads, fatigue, aging and natural disasters. Accordingly, diagnostic methods for damage assessment have been developed and implemented, aiming to assess the impending failure. To this end, the Acoustic Emissions (AE) technique was developed and is being improved continuously in order to provide a useful tool for monitoring and understanding the mechanisms of dynamic processes, but also for warning of upcoming failure [1]. Acoustic Emission events occur due to sudden release of mechanical energy in the form of short mechanical vibrations due to the fact that a material is under mechanical loading. This mechanical vibration travels in the form of spherical waveforms through the material's bulk. The AE event analysis is used to estimate the damage degree when brittle materials such as concrete and rocks are subjected to mechanical loading [2-5].
Acoustic Emission (AE) due to crack growth in brittle materials is usually observed in the high frequency range, typically between 50 kHz and 800 kHz. AE are recorded even from the early stages of the damage process. During the fracture process in quasi-brittle materials, the micro cracks formation and growth are manifested by a number of AE events released at different amplitudes. It has been shown that as a specimen under mechanical loading approaches failure, there is

an increase in the AE activity rate, as a result of the deterioration of the mechanical properties. Particularly in cement based materials and concrete structures the AE testing is one of the most widely used methods for monitoring crack growth [1].
Another phenomenon related to the micro-crack growth in quasi-brittle nonmetallic materials is the production of electric charges that shape electric dipoles forming a rather complicated charge system [6-8]. Such electric dipoles produce an electric potential across a crack resulting in the appearance of an electric current [9]. Such currents have been measured in both laboratory [7, 10] and at a geodynamic scale [11] and their detection may be useful as a precursor of a fracture.
These electrical signals (weak electrical current emissions) are detected using a novel experimental technique, called Pressure-Stimulated Currents Technique, and the recorded electrical currents are described by the term Pressure Stimulated Currents (PSC) [12]. The PSC's are weak electric currents detected with sensitive electrometers when a pair of electrodes is attached at proper locations on the specimen that is subjected to mechanical stress. Initially, the PSC technique was applied when rock specimens like marble [6, 13] and amphibolite [14] were subjected to compressive axial stress increasing up to failure. Consequently, it was successfully applied to cement-based materials [15, 16]. The PSC technique was also tested during laboratory experiments of three-point bending (3PB) tests on marble [17] and cement-based specimens [5]. The PSC technique has been adopted by several researchers [9, 18], while others use similar techniques [19-21].
Both AE and PSC signals provide important information about the damage processes occurring in specimens under compression or under bending tests. In particular, the PSCs show a considerable increase when the applied load reaches the vicinity of failure and attain their peak value shortly before failure [12, 13, 15, 16].
In Acoustic Emissions one of the statistical parameters, which is often used to estimate a critical situation, is the b-value [1, 22, 23], which exhibits systematic variations during the different stages of fracture processes. The AE based b-value analysis and the variation of the b-value, have attracted researchers working in the engineering field [23, 24]. Other AE statistical parameters that have been used include the event and energy release rates, the cumulative energy and the ring down counts.
In this paper attention is focused on the parallel presentation of AE and PSC detected during 3PB of cement mortar specimens. The main difference between the three experiments is the loading mode. Specifically, one test was conducted under a constant loading rate (i.e. linear load increase) up to fracture while at the other two experiments the load was increasing according to a non-linear mode.

EXPERIMENTAL DETAILS

The specimens used for the experiments were prismatic cement mortar beams with dimensions 250x50x50 mm^3. Their bending strength (L_f) varied from 3.5kN to 4.0kN. Details regarding the specimens, the preparation process and the experimental apparatus can be found in a previous work [25].
Contrary to previous publications [25], the electrodes that were used to capture the PSC emissions were placed as shown in Fig. 1, i.e. on the lower side of the beam (tension zone) and at the left and right sides, symmetrically with respect to the specimen's central cross section where the load is applied. This topology was decided after several experiments conducted in order to estimate the best installation process that ensures the recording of strong PSCs and limits the influence of electric noise. The best electrode distance (ℓ) was also investigated and it was empirically found that for the specific type of experiments it should be $\ell \approx \alpha / 5$, where α is the distance between the two rigid metallic cylindrical rods used to support the cement beam. The PSC was captured by the electrodes and measured using a high sensitivity electrometer (Keithley, model 6517). The data were recorded in real time and stored on a hard disk through a GPIB interface. The mechanical load applied was recorded with the use of an analog-to-digital (A/D DAQ) data acquisition device (Keithley model KUSB-3108). The whole setup was placed in a Faraday shield in order to avoid interference from external electrical noise.
The system that was used to detect and record the AE is the 2-channel PCI-2 AE acquisition system (Physical Acoustics Corp). The R15a sensor (manufactured by PAC, resonant at 75 kHz) was placed in the middle of the beam (see Fig. 1) in order to focus on the region of the crack development processes that take place due to the externally applied bending load. The sensor was coupled to the test specimen using vacuum grease. Preamplifier was used along with the sensor with gain set at 40dB. The signals were band-pass filtered between 20-400 kHz using the software control of the data acquisition system. To set the threshold value for recording and to ensure that sensors were correctly performing, pencil lead breaks (5mm, HB leads) were carried out near the crack tip and the recorded signals were observed. The value of 40dB was selected since it was found to prevent the recording of lower amplitude reflected signals from the pencil lead break tests. For the detected AE data processing the Physical Acoustics Corp. Noesis software was used.

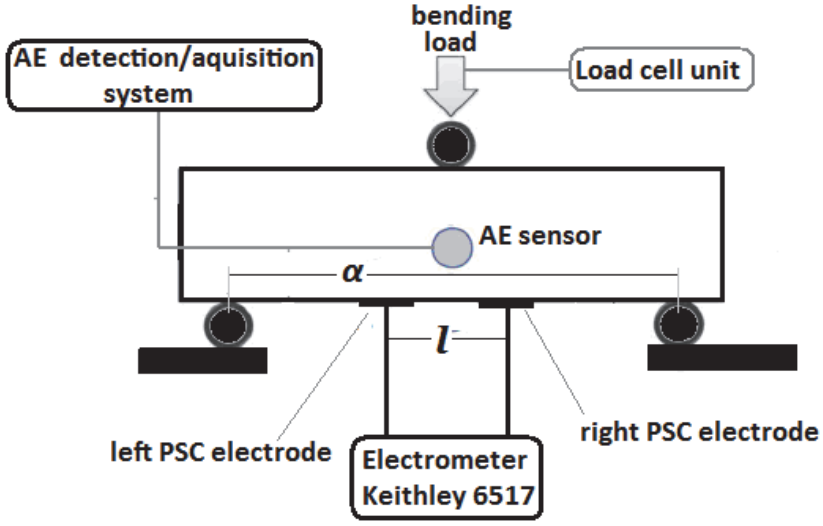

Figure 1: The experimental installation and the location of the AE and PSC sensors.

RESULTS AND DISCUSSION

Tab. 1 includes all the details regarding the loading protocol of each specimen for the three experiments implemented, i.e. load (L) vs. time (t), considering that the function is best described as:

$$L(t) = C_1 \cdot t^2 + C_2 \cdot t \quad (1)$$

where C_1 and C_2 are constants. During the first experiment (i.e. specimen CB01) a linear increase of the load was conducted at a rate of 100N/s while the two following experiments were conducted following a non-linear increase of the mechanical load (see Tab. 1).

Specimen	$L(t) = C_1 \cdot t^2 + C_2 \cdot t$	L_f (kN)	PSC_{peak} (pA)	Q_T (pC)	AE hits	Cum. Energy AE
CB01	C_1=0, C_2=+100N/s	3.6	28.8	294	1062	5.17x10^7 aJ
CB02	C_1=-7.3N/s^2, C_2=+333N/s	3.8	27.2	298	543	4.50x10^7 aJ
CB03	C_1=+0.7N/s^2, C_2=35.4N/s	3.5	29.9	291	893	4.98x10^7 aJ

Table 1. The characteristics of the loading protocol followed during each of the three experiments conducted and the main quantities studied regarding the PSC and AE recordings.

Fig. 2 shows the temporal variation of the emitted PSC from the three experiments, as well as the corresponding behavior of the mechanical load. Shortly before failure of the specimens the emitted PSC tends to show a peak. The recorded peak value (PSC_{peak}) is similar in all three experimental loading protocols (see Tab. 1). The fact that the PSC is maximized before the failure of the cement mortar beam has been systematically observed during compressive stress tests on both cement based [15] and rock [26, 27] materials. This behavior is best demonstrated by the specimen CB02. This is attributed to the fact that the specimen approaches failure at the lowest load rate (see blue lines in Fig. 2). The level of the bending load, for which the PSC signal begins to show an intense and continuous increase, irrespectively of the loading mode, is estimated to be at approximately 60% of the ultimate 3PB strength (L_f) (see Fig. 3), in all three experiments.

As a next step, it is interesting to consider the total electric charge (Q_T), released during the three experiments up to failure. The Q_T was calculated using the relation (t_f is the failure time).

$$Q_T = \int_0^{t_f} PSC(t)\,dt \tag{2}$$

It is worth mentioning that the total electric charge for the three different loading modes reaches almost the same value (see Tab. 1). In a previous work [13], during compressive stress application on marble specimens it was theoretically supported and experimentally proven [28] that the total electric charge value does not depend on the applied mechanical stress rate. This behavior is verified experimentally herein when cement mortar specimens are subjected to 3PB loading.

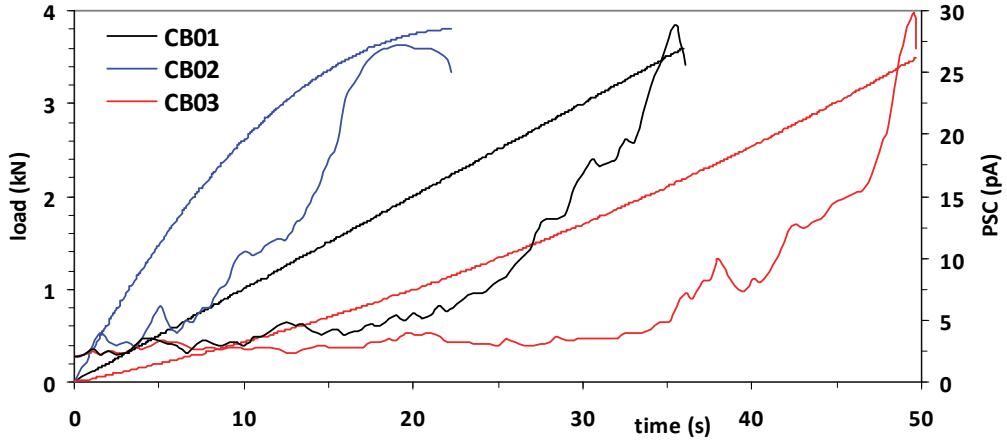

Figure 2: The time variation of the applied 3PB load and the corresponding time variation of the PSC, during all three experiments conducted.

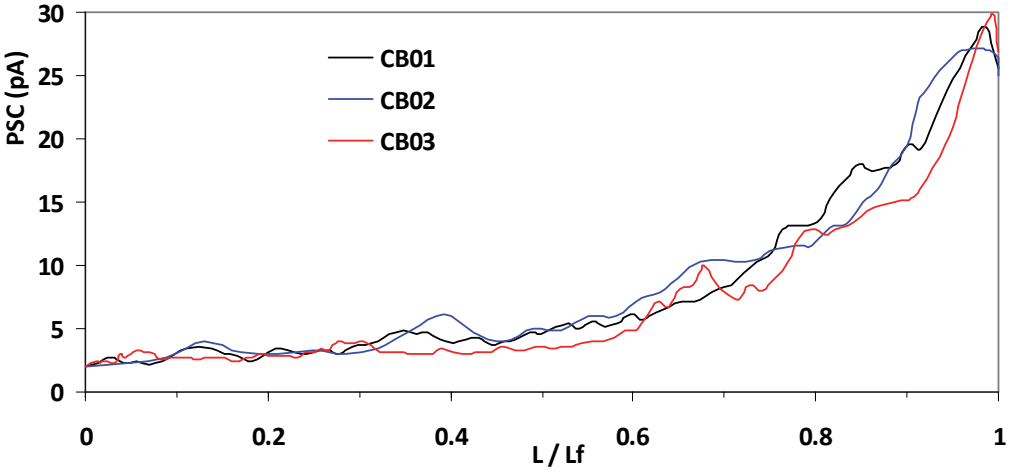

Figure 3: PSC versus normalized load (L/L_f) for all three experiments conducted.

Regarding the AE recordings, during the three experiments, a different number of AE hits was recorded (see Tab. 1). The micro-cracks generated during loading are of different sizes and therefore different AE amplitudes are recorded. A common way of obtaining quantitative information from the above statements is by computing the b-value of AE using the methods adopted in seismology [29, 30]. The b-value is defined as the log-linear slope of the frequency–magnitude distribution of AE [31]. In the present study, the b-values were calculated by applying a method that is known as improved b-value (I_b) analysis after Shiotani et al. [32]. The I_b-value is defined as:

$$I_b = \frac{\log N(\mu - \alpha_1\sigma) - \log N(\mu + \alpha_2\sigma)}{(\alpha_1 + \alpha_2)\cdot\sigma} \tag{3}$$

where, σ is the standard deviation of the magnitude distribution in one group of events, μ is the mean value of the magnitude distribution in the same group of events, and α_1 as well as α_2 are constants, for which usually a value equal to 1 is adopted [1].

In order to highlight the variability of the I_b-value, during the three experiments, the b-value analysis of AE is, in general, applied to a certain number of events, as follows: from event 1 to n, then from event 2 to n+1, and so on. The determination of the value of n has been considered by Shiotani et al. [32] and Colombo et al. [22], since it constitutes a parameter that can influence the results. A value exceeding n=50 is assumed to be a satisfactory one. In the present study, n=70 has been selected. Each value of I_b was calculated from a group of the events 1 to 70, consequently from 2 to 71, and so on. Each calculated I_b value is associated to the time of the 70th event of each group and to that of the corresponding value of normalized (L/L_f) load. The variability of the I_b-value during the three experiments with respect to the normalized (L/L_f) load is shown in Fig. 4. In the same figure the corresponding variation of PSC signals is also presented.

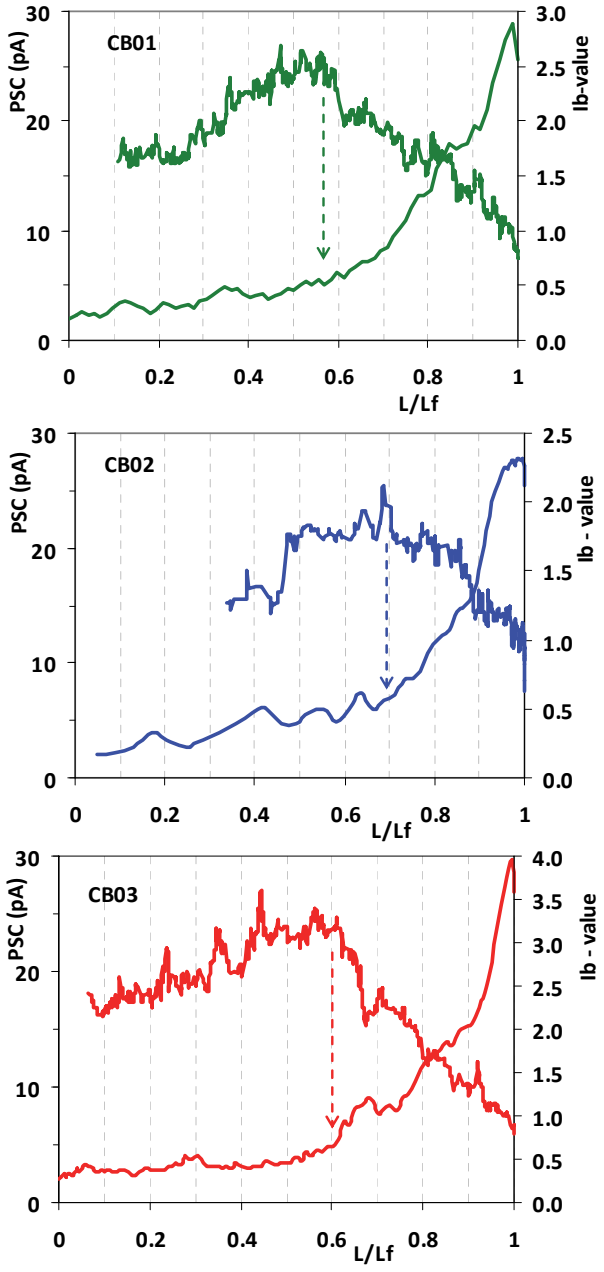

Figure 4: Variation of I_b-values and PSC signals vs. normalized load (L/L_f) for the three conducted experiments.

It is obvious that during the early stages ($L<0.6L_f$ approximately), the I_b-values show an almost constant increase indicating the prevalence of micro-cracking [33]. In these stages the PSC signal is low, showing a slight increase (see Fig. 4). Then, at the following stages ($L>0.6L_f$) I_b-values show an intense reduction combined with a sharp increase of the PSC. This behavioral change in the variability of the I_b-value is observed at a critical normalized load value $[L/L_f]_C \approx 0.6$, for all three experiments. As it is marked in Fig. 4 (dotted arrows), the exact value $[L/L_f]_C$ is 0.55, 0.62 and 0.70 for specimens CB01, CB02 and CB03, respectively. It seems that increasing the rate of the applied bending load the increase of the PSC signal and the corresponding reduction of I_b-values are recorded earlier. It should be pointed out that the I_b-value fluctuation, which is observed in all three experiments at the early stage, is related to the fact that the micro-cracks begin to form randomly. Moreover, in all three experiments, I_b attains values around 1 during the last seconds before the failure of the specimens, which is indicative of the final formation of a localized macro-crack.

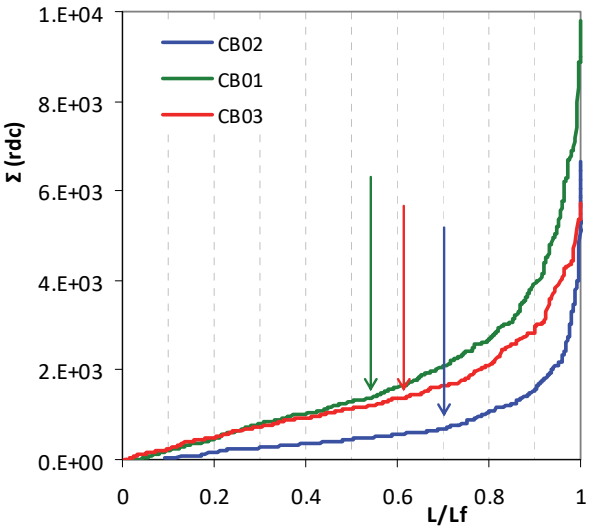

Figure 5: The cumulative ring down count of AE hits vs. normalized load (L/L_f) for the three conducted experiments.

The ring down count (rdc) data was also used, since it is a measure of the number of AE waveform oscillations through a preset voltage threshold [1]. In order to highlight the identification and assessment of important stages of micro-crack damage in a cement mortar material, a common practice has been followed to examine the cumulative ring down count Σ(rdc) and energy (ΣE). These results are illustrated in Figs. 5 and 6 with respect to the normalized load (L/L_f). In all three experiments an almost constant increase in Σ(rdc) was initially observed, related to the initiation of new micro-cracks. For $L/L_f > [L/L_f]_C$ the Σ(rdc) increases at a rate indicating the development of severe damage in the specimen. Concurrently, an abrupt increase of the PSC signal is observed.

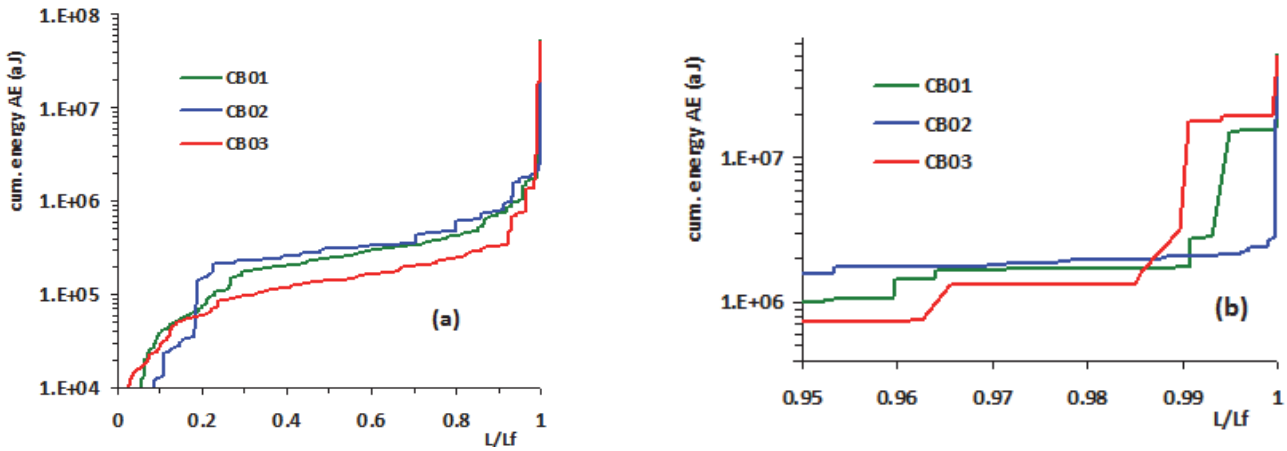

Figure 6: (a) The cumulative AE energy vs. normalized load (L/L_f) for the three experiments and (b) a detailed view close to the fracture load.

Finally, the cumulative energy of the AE hits up to the fracture of the specimens for all three experiments versus the normalized load level (L/L_f) is plotted in Fig. 6a. A significant step-up increase of the cumulative AE energy is observed slightly before the failure of the specimens (see the detailed view in Fig. 6b). The corresponding values of the cumulative energy practically start to converge (see Tab. 1).

CONCLUDING REMARKS

The application of 3PB loading under various protocols regarding the bending load rate on cement mortar beams causes the emission of electric currents (PSC) that show a clearly deterministic behavior. The total electric charge recorded during each experimental procedure is practically of similar value for all three experiments. It may be concluded that the corresponding behavior of the studied AE parameters is also similar.

Micro-cracks generate a sufficient number of weak acoustic emissions leading to a relatively high b-value. When increasing load levels, the fracture process moves from micro- to macro-cracking and the I_b-value decreases.

A distinct correlation between the PSC and the calculated I_b values is observed. Specifically, when I_b-values are relatively high and tend to increase, the PSC signals also exhibit a smooth increase. When I_b-values progressively decrease, the PSC signals show intense increase, indicating that PSC emissions are mainly attributed to crack formation and propagation. The peak of the PSC signals is another clear indication of the upcoming failure. Finally, the damage initiation is also verified by the study of the cumulative ring down count. The qualitative similarity of the results of the present protocol with recently published ones for natural stones and especially for Dionysos marble [17], which is the material extensively used for the restoration of marble monuments in Greece [34-38], supports further the potential use of the PSC technique for in-situ monitoring the response of restored structural elements of masterpieces of Cultural Heritage.

REFERENCES

[1] Rao, M.V.M.S., Lakschmi, P.K.J. Analysis of *b*-value and improved b-value of acoustic emissions accompanying rock fracture. Current Science, 89 (2005) 1577-1582.

[2] Aggelis D.G., Mpalaskas A.C., Matikas T.E., Investigation of different fracture modes in cement-based materials by acoustic emission, Cement and Concrete Research, 48 (2013) 1–8

[3] Stanchits, S., Dresen, G., Vinciguerra, S., Ultrasonic velocities, acoustic emission characteristics and crack damage of basalt and granite, Pure Applied Geophys,163 (2006) 5–6, 975–994

[4] Lockner, D., The role of acoustic emission in the study of rock fracture. Int. J. Rock Mech. Min. Sci. Geomech. Abstr., 30 (1993) 883–899.

[5] Stergiopoulos, C., Stavrakas, I., Hloupis, G., Hloupis, D., Triantis, Vallianatos, F., Electrical and acoustic emissions in cement mortar beams subjected to mechanical loading up to fracture, Engineering Failure Analysis, 35 (2013) 454-461.

[6] Stavrakas, I., Anastasiadis, C., Triantis, D., Vallianatos, F., Piezo Stimulated currents in marble samples: Precursory and concurrent – with – failure signals, Natural Hazards and Earth System Sciences, 3 (2003) 243-247.

[7] Vallianatos, F., Triantis, D., Tzanis, A., Anastasiadis, C., Stavrakas, I., Electric Earthquake Precursors: From Laboratory Results to Field Observations, Physics and Chemistry of the Earth, 29 (2004) 339-351.

[8] Varotsos, P.A., Sarlis, N.V., Skordas, E.S., Long-range correlations in the electric signals that precede rupture, Phys. Rev. E, 66 (2002) 011902.

[9] Cartwright-Taylor, A., Vallianatos, F., Sammonds, P., Superstatistical view of stress-induced electric current fluctuations in rocks, Physica A: Statistical Mechanics and its Applications, 414 (2014) 368–377.

[10] Frid, V., Goldbaum, J., Rabinovitch, A., Bahat, D., Electric polarization induced by mechanical loading of Solnhofen limestone, Phil. Mag. Lett., 89 (7) (2009) 453–463

[11] Varotsos, P.A., The Physics of Seismic Electric Signals, TerraPub (2005)

[12] Stavrakas, I., Triantis, D., Agioutantis, Z., Maurigiannakis, S., Saltas, V., Vallianatos, F., Pressure Stimulated Currents in rocks and their correlations with mechanical properties, Natural Hazards and Earth System Sciences, 4 (2004) 563-567.

[13] Triantis, D., Stavrakas, I., Anastasiadis, C., Kyriazopoulos, A., Vallianatos, F., An analysis of Pressure Stimulated Currents (PSC), in marble samples under mechanical stress, Physics and Chemistry of the Earth, 31 (2006) 234-239.

[14] Triantis, D., Anastasiadis, C., Vallianatos, F., Kyriazis, P., Nover, G., Electric signal emissions during repeated abrupt uniaxial compressional stress steps in amphibolite from KTB drilling, Natural Hazards & Earth System Sciences, 7 (2007) 149-154.
[15] Kyriazopoulos, A., Anastasiadis, C., Triantis, D., Brown, J. C, Non-destructive evaluation of cement-based materials from pressure-stimulated electrical emission - Preliminary results, Construction and Building Materials, 25 (2011) 1980-1990.
[16] Triantis, D., Stavrakas, I., Kyriazopoulos, A., Hloupis, G., Agioutantis, Z., Pressure Stimulated Electrical Emissions from cement mortar used as failure predictors, International Journal of Fracture, 175 (2012) 53-61.
[17] Stavrakas, I., Pasiou, E.D., Hloupis, G., Malliaros, G.-T., Triantis, D., Kourkoulis, S.K., Exploring the size effect of marble by combined use of Pressure Stimulated Currents and Acoustic Emission, in: Beskos D.E., Stavroulakis G.E. (Eds.), 10th HSTAM International Congress on Mechanics, Chania, Hellas, (2013) 185-186.
[18] Li, Z., Enyuan, W., Miao, H., Laboratory Studies of Electric Current Generated during Fracture of Coal and Rock in Rock Burst Coal Mine, Journal of Mining, 2015 (2015) ID 235636.
[19] Sun, M., Liu, Q., Li, Z., Wang, E. Electrical emission in mortar under low compressive loading. Cement and Concrete Research, 32 (2002) 47–50.
[20] Archer, J. W., Dobbs, M. R., Aydin, A., Reeves, H. J., & Prance, R. J., Measurement and correlation of acoustic emissions and pressure stimulated voltages in rock using an electric potential sensor. International Journal of Rock Mechanics and Mining Sciences, 89 (2016) 26-33.
[21] Dann, D., Demikhova, A., Fursa, T., Kuimova, M., Research of Electrical Response Communication Parameters on the Pulse Mechanical Impact with the Stress–Strain State of Concrete Under Uniaxial Compression, IOP Conf. Series: Materials Science and Engineering, 66 (2014) 012036. doi:10.1088/1757-899X/66/1/012036
[22] Colombo, S., Main, I., G., Forde, M. C., Assessing damage of Reinforced Concrete Beam using "*b*-value" Analysis of Acoustic Emission signals. J. Mat. Civil Eng. (ASCE), 15 (2003) 280-286.
[23] Vidya Sagar, R., Prasad, RV., Raghu Prasad, B.K., Rao, M.V.M.S., Microcracking and fracture process in cement mortar and concrete: a comparative study using acoustic emission technique. Experimental Mechanics, 53 (2013) 1161–1175.
[24] Vidya Sagar, R., Raghu Prasad, B.K., Shantha Kumar, S., An experimental study on cracking evolution in concrete and cement mortar by the b-value analysis of acoustic emission technique, Cement and Concrete Research, 42 (2012) 1094-1104.
[25] Stergiopoulos, C., Stavrakas, I., Hloupis, G., Triantis, D., Vallianatos, F., Electrical and acoustic emissions in cement mortar beams subjected to mechanical loading up to fracture, Engineering Failure Analysis, 35 (2013) 454–461.
[26] Anastasiadis, C., Stavrakas, I., Triantis, D., Vallianatos, F., Correlation of pressure stimulated currents in rocks with the damage variable, Annals of Geophysics, 50 (2007) 1-6.
[27] Vallianatos, F., Triantis, D., Scaling in Pressure Stimulated Currents related with Rock Fracture, Physica A, 387 (2008) 4940-4946.
[28] Triantis, D., Anastasiadis, C., Stavrakas, I., The correlation of electric charge with strain on stressed rock samples, Natural Hazards and Earth System Sciences, 8 (2006) 1243-1248.
[29] Scholz, C. H., The frequency–magnitude relation of microcracking in rock and its relation to earthquakes. Bull. Seis. Soc. Am., 58 **(**1968) 399–415.
[30] Aki, K., Maximum likelihood estimates of *b* in the formula log*N* = *a* – *bm* and its confidence limits. Bull. Earthquake Res. Inst., Tokyo Univ., 43 **(**1965) 237–239.
[31] Main, I. G., Meredith, P. G. and Jones, C., A reinterpretation of the precursory seismic *b*-value anomaly from fracture mechanics. Geophys. J., 96 (1989) 131–138.
[32] Shiotani, T., Yuyama S., Li, Z. W., Ohtsu, M. Application of the AE improved b-value to qualitative evaluation of fracture process in concrete materials, J. Acoust. Emission, 19 (2001) 118–132.
[33] Rouchier, S., Foray, G., Godin, N., Woloszyn, M., Roux, J.-J. Damage monitoring in fibre reinforced mortar by combined digital image correlation and acoustic emission, Construction and Building Materials, 38 (2012) 371-380.
[34] Kourkoulis, S.K., Ganniari-Papageorgiou, E., Mentzini, M., Dionysos marble under bending: A contribution towards understanding the fracture of the Parthenon architraves, Engineering Geology, 115 (3-4) (2010) 246-256.
[35] Kourkoulis, S.K., Prassianakis, I., Agioutantis, Z., Exadaktylos, G.E., Reliability assessment of the NDT results for the internal damage of marble specimens, International Journal of Material and Product Technology, 26(1/2) (2006) 35-56.
[36] Kourkoulis, S.K., Exadaktylos, G.E., Vardoulakis I., U-notched Dionysos-Pentelicon marble in three point bending: The effect of nonlinearity, anisotropy and microstructure, International Journal of Fracture, 98(3-4) (1999) 369-392.

[37] Exadaktylos, G.E., Vardoulakis, I., Kourkoulis S.K., Influence of nonlinearity and double elasticity on flexure of rock beams – II. Characterization of Dionysos marble, International Journal of Solids and Structures, 38(22-23) (2001) 4119-4145.
[38] Kourkoulis, S.K., Pasiou, E.D., Interconnected epistyles of marble monuments under axial loads', International Journal of Architectural Heritage, 9(3) (2015) 177–194.